

Dileptons from correlated D- and \bar{D} -meson decays in the invariant mass range of the QGP thermal radiation using the UrQMD hybrid model

Thomas Lang^{1,2}, Hendrik van Hees^{1,2}, Jan Steinheimer³, and Marcus Bleicher^{1,2}

¹ *Frankfurt Institute for Advanced Studies (FIAS),
Ruth-Moufang-Str. 1, 60438 Frankfurt am Main, Germany*

² *Institut für Theoretische Physik, Johann Wolfgang Goethe-Universität,
Max-von-Laue-Str. 1, 60438 Frankfurt am Main, Germany and*

³ *Lawrence Berkeley National Laboratory,
1 Cyclotron Road, Berkeley, CA 94720, USA*
(Dated: February 9, 2021)

Abstract

Relativistic heavy-ion collisions produce a hot and dense thermalized medium, that is expected to emit thermal radiation in form of dileptons. These dileptons are not affected by the strong force and are therefore a clean probe for the possible creation of a Quark Gluon Plasma (QGP). However, electroweak decays of open-charm mesons are expected to induce a substantial background in the invariant mass region between the ϕ and J/Ψ peak ($1 \text{ GeV} \lesssim M_{\ell^+\ell^-} \lesssim 3 \text{ GeV}$) of the thermal QGP radiation. To evaluate this background radiation we apply a Langevin approach for the transport of charm quarks in the UrQMD (hydrodynamics + Boltzmann) hybrid model. Due to the inclusion of event-by-event fluctuations and a full (3+1)-dimensional hydrodynamic evolution, the UrQMD hybrid approach provides a more realistic model for the evolution of the matter produced in heavy ion collisions as compared to simple homogeneous fireball expansions usually employed before. As drag and diffusion coefficients we use a resonance approach for elastic heavy-quark scattering and assume a decoupling temperature of the charm quarks from the hot medium of 130 MeV. For the hadronization of the charm quarks we employ a coalescence approach at the decoupling temperature from the medium. In this letter we present our calculations of the D-meson correlations and the invariant mass spectra of the dilepton decays in heavy-ion collisions at FAIR, RHIC, and LHC energies using different interaction scenarios.

I. INTRODUCTION

In the spirit to explore the possible existence of a phase of matter with quarks and gluons as degrees of freedom, the Quark Gluon Plasma (QGP), various attempts have been made to propose observables for its verification [1–3].

One particularly interesting probe for the exploration of the QGP are charm quarks. Charm quarks are produced in the hard primary parton-parton collisions in the pre-equilibrium phase of the matter evolution. Since the quantum number charm is conserved in the strong interaction, charm quarks are produced as charm-anti-charm pairs and are emitted dominantly back-to-back due to momentum conservation. In the following evolution of the (locally thermalized) medium, the charm quarks traverse the QGP and finally hadronize to D/ \bar{D} -mesons when the system cools down. These D/ \bar{D} -mesons decay to electrons and positrons and can be measured. The angular correlations between the decaying D/ \bar{D} -mesons lead to correlated e^+e^- -pairs which populate the invariant-mass spectra. Depending on the strength of the medium interaction of the D/ \bar{D} -mesons and their momentum change during the hadronization process a different strength in the angular correlations have already been explored in [4, 5] using a Langevin approach on a Bjorken’s hydrodynamics background. In this study a substantial modification of the correlations distributions in the partonic phase was found. The modification in the hadronic phase, however, seems to be negligible.

Apart from learning more about D-meson interactions in the medium, such calculations can also be utilized to learn more about thermal QGP radiation. Thermal dilepton radiation of the hot and dense matter allows to draw conclusions on the matters nature, i.e., to determine its temperature and the in-medium properties of the electromagnetic current correlation function, which is closely related to the spectral properties of the light vector mesons, ρ , ω , and ϕ , in the low-mass region, $M_{\ell+\ell^-} \lesssim 1$ GeV [6–8]. Unfortunately though, background radiation complicates these measurements. By far, the most important contribution to this background radiation in the invariant-mass range between the ϕ and J/Ψ peak of approximately 1 GeV to 3 GeV is the dilepton radiation originating from open-charm decays, where it competes with the thermal radiation from the partonic phase of the fireball evolution. This background yield is sensitive to the energy loss of charm quarks in the medium. Thus, the knowledge of charm quark and D-meson interactions in the hot medium provides us with insights to the thermal QGP radiation.

In this paper we explore the D-meson correlations and the invariant mass spectra of D-meson dileptons at FAIR (Au+Au at a beam energy of $E_{\text{lab}} = 25$ GeV), RHIC (Au+Au at $\sqrt{s_{NN}} = 200$ GeV) and LHC (Pb+Pb at $\sqrt{s_{NN}} = 2.76$ TeV). For this purpose we use a hybrid model, consisting of the Ultra-relativistic Quantum Molecular Dynamics (UrQMD) model [9, 10] and a full (3+1)-dimensional ideal hydrodynamical model [11, 12] to simulate the bulk medium. The heavy-quark propagation in the medium is described by a relativistic Langevin approach.

Similar quark-propagation studies have recently been performed in a thermal fireball model with a combined coalescence-fragmentation approach from Rapp and Hees [13–19], in an ideal hydrodynamics model with a lattice-QCD EoS [20, 21], in a model from Kolb and Heinz [22], in the BAMPS model [23, 24], the MARTINI model [25] as well as in further studies and model comparisons [26–30]. Previous studies, that focus on the correlation of D-mesons and/or invariant mass spectra in transport models, can be found in [4, 5, 31–33].

The UrQMD hybrid model provides a realistic and well established background, including event-by-event fluctuations and has been shown to very well describe many collective properties of the hot and dense medium created in relativistic heavy-ion collisions.

II. DESCRIPTION OF THE MODEL

The UrQMD hybrid model [34] combines the advantages of transport theory and (ideal) fluid dynamics. The initial conditions are generated by the UrQMD model [10, 35, 36], followed by a full (3+1)-dimensional ideal fluid dynamical evolution, including the explicit propagation of the baryon current. After a Cooper-Frye transition back to the transport description, the freeze out of the system is treated dynamically within the UrQMD hadron cascade. The hybrid model has been successfully applied to describe particle yields and transverse dynamics from AGS to LHC energies [34, 37–40] and is therefore a reliable model for the flowing background medium.

The equation of state includes quark and gluonic degrees of freedom coupled to a hadronic parity-doublet model [41]. It has a smooth crossover at low baryon densities between an interacting hadronic system and a quark gluon plasma and a first order phase transition at higher densities. The thermal properties of the EoS are in agreement with lattice QCD results at vanishing baryon density.

For the present study of the charm quark dynamics in the expanding medium of light quarks we employ the well-known stochastic Langevin equation, suitable for numerical simulations [13, 26, 42–46]. Such a Langevin process reads

$$dx_j = \frac{p_j}{E} dt, \quad dp_j = -\Gamma p_j dt + \sqrt{dt} C_{jk} \rho_k. \quad (1)$$

Here $E = \sqrt{m^2 + \mathbf{p}^2}$, and Γ is the drag or friction coefficient. The covariance matrix, C_{jk} , of the fluctuating force is related with the diffusion coefficients. Both coefficients are dependent on $(t, \mathbf{x}, \mathbf{p})$ and are defined in the (local) rest frame of the fluid. The ρ_k are Gaussian-normal distributed random variables. For details, the reader is referred to [19, 47].

The drag and diffusion coefficients for the heavy-quark propagation within this framework are taken from a resonance approach [44, 47]. It is a non-perturbative approach, where the existence of D-mesons and B-mesons in the QGP phase is assumed. The drag and diffusion coefficients obtained from this approach are shown in Figure 1 (left) as function of the three-momentum $|\vec{p}|$ at $T = 180$ MeV and in Figure 1 (right) as function of the temperature at a fixed three-momentum of $|\vec{p}| = 0$.

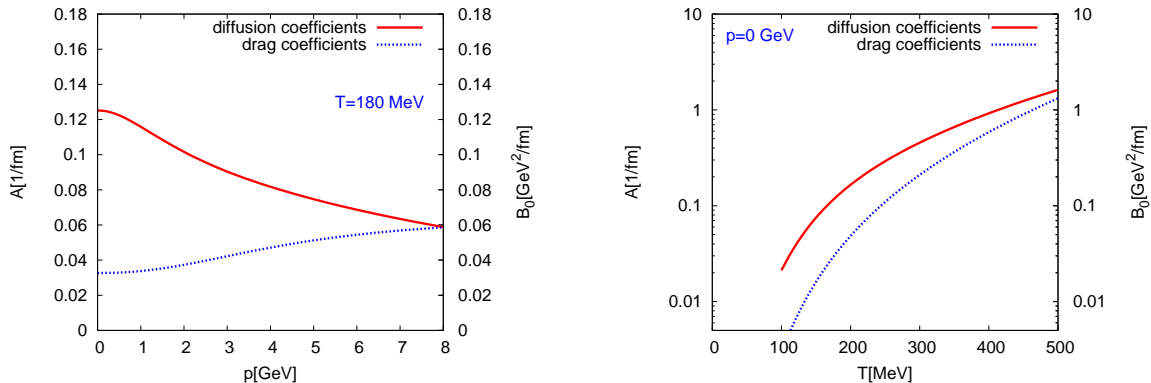


FIG. 1. (Color online) Drag and diffusion coefficients in the resonance model for charm quarks. Left: The plot shows the dependence of the coefficients on the three-momentum $|\vec{p}|$ at a fixed temperature of $T = 180$ MeV. Right: The plot shows the dependence of the coefficients on the temperature at a fixed three-momentum $|\vec{p}| = 0$.

The initial production of charm quarks in our framework is based on a time resolved “Glauber” approach [48–51], i.e. we perform first a UrQMD run excluding interactions between the colliding nuclei and save the nucleon-nucleon collision space-time coordinates. These coordinates are used in a second, full UrQMD run as (possible) production space-time coordinates for the charm quarks.

For the initially produced charm quarks at FAIR, RHIC and LHC energies we utilize different models:

- For collisions at $E_{\text{lab}} = 25 \text{ AGeV}$ we use the D-meson transverse mass spectrum from HSD calculations [52] fitted by

$$\frac{dN}{dp_T} = \frac{C}{(1 + A_1 \cdot p_T^2)^{A_2}}, \quad (2)$$

with the coefficients $A_1 = 0.870/\text{GeV}^2$ and $A_2 = 3.062$. C is an arbitrary normalization constant with the unit $1/\text{GeV}$. This function is then used for the initial charm quark production.

- At RHIC ($\sqrt{s_{NN}} = 200 \text{ GeV}$) we use

$$\frac{dN}{dp_T} = \frac{C \cdot (1 + A_1 \cdot p_T^2)^2 p_T}{(1 + A_2 \cdot p_T^2)^{A_3}}, \quad (3)$$

with $A_1 = 2.0/\text{GeV}^2$, $A_2 = 0.1471/\text{GeV}^2$, $A_3 = 21.0$. C is an arbitrary normalization constant with the unit $1/\text{GeV}^2$. This distribution is taken from [13, 44]. It is obtained by using tuned c-quark spectra from PYTHIA. Their pertinent semileptonic single-electron decay spectra account for pp and dAu measurements by the STAR collaboration up to $p_T = 4 \text{ GeV}$. The missing part at higher p_T is then supplemented by B-meson contributions.

- At LHC ($\sqrt{s_{NN}} = 2.76 \text{ TeV}$) the initial distribution is obtained from a fit to PYTHIA calculations. The fitting function we use is

$$\frac{dN}{dp_T} = \frac{C p_T}{(1 + A_1 \cdot p_T^2)^{A_2}}, \quad (4)$$

with the coefficients $A_1 = 0.379/\text{GeV}^2$ and $A_2 = 5.881$. C again is an arbitrary normalization constant with the unit $1/\text{GeV}^2$. In all cases we neglect gluon radiation on the outgoing charm quarks and assume a full back-to-back emission of the $c\bar{c}$ pair.

Starting with these charm-quark distributions as initial conditions we perform in the hydrodynamic state an Ito post-point time-step of the Langevin simulation, employing the local hydro’s cell velocities and cell temperatures for the calculation of the momentum transfer to the heavy quarks.

We include a hadronization mechanism for charm quarks into D-Mesons, via the use of a quark-coalescence mechanism (see [47, 53–55] for details) when the decoupling temperature is reached.

This approach has already been successfully applied to describe experimental measurements of the nuclear modification factor and the elliptic flow at RHIC and LHC energies [47, 53, 54]. Moreover it has been used to predict the medium modification of D-mesons at FAIR energies [55].

III. THE CORRELATION-ANGLE DISTRIBUTION

Let us start with our results for the azimuth angular correlation, followed by the full angular correlation. We have performed our calculations for FAIR, RHIC and LHC energies in the centrality range of $\sigma/\sigma_{\text{tot}} = 20\%-40\%$. Our results for the relative azimuth correlation of the decoupled D-mesons, that means the azimuth angle of the momenta between quark pairs emitted back-to-back, are shown in Fig. 2.

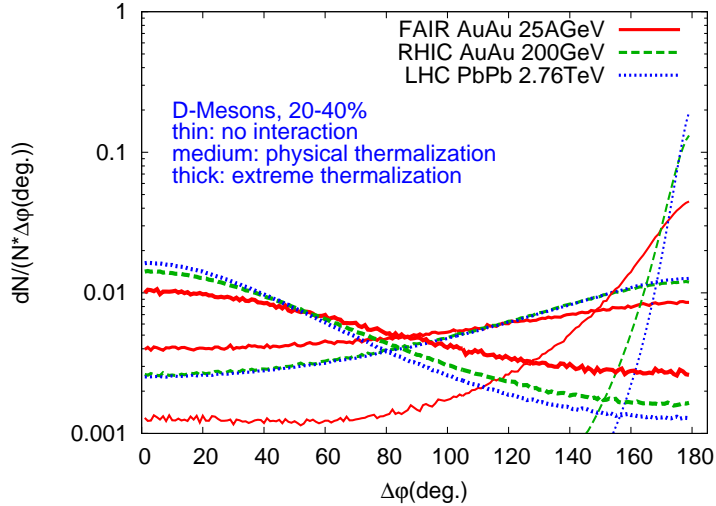


FIG. 2. (Color online) Relative azimuth correlations of D-mesons at FAIR, RHIC and LHC energies in the centrality range of 20-40%. Three different scenarios are shown: no interaction with the medium, physical drag and diffusion coefficients and extreme thermalization with 20-fold higher coefficients. The angular modification for the case of no interaction with the medium is due to the coalescence mechanism. The yields are normalized to one.

The following observations can be made:

No interaction: The charm quarks do not interact with the medium. The modification of the initial back-to-back correlation is due to the coalescence mechanism only. We observe that the coalescence alone leads to a considerable modification of the $D\bar{D}$ angular distribution. This modification grows larger for lower energies since the charm momenta are lower and the modification due to the coalescence with the light quarks is relatively more important.

Physical scenario: We apply the full calculation plus coalescence, which has been successful in describing R_{AA} and v_2 of non-photonics electrons at RHIC as well as D-mesons at the LHC [47, 53, 54]. Here the angular distribution flattens and virtually all charm quarks interact considerably with the hot medium. The distribution for charm quarks at RHIC and LHC energies does hardly differ while the modification at FAIR energies is somewhat larger due to the slower medium evolution and the stronger modification due to the coalescence mechanism. This finding is in agreement with the calculations of [4].

Extreme heavy-quark thermalization: For this scenario the drag and diffusion coefficients are multiplied by a factor of 20. Therefore the charm quarks become nearly completely thermalized with the bulk medium. The charm quarks tend to adopt angular correlations diametrically opposed to the initial correlations. This is different from the calculated “flat” correlation distribution for full thermalization in [4]. This difference is due to the radial and elliptic flow which has been neglected in the calculation of [4], but is included in our full (3+1)-dimensional hydrodynamic evolution. Charm and anti-charm-quarks which are initially produced back-to-back are dragged

with the expanding medium and their angles align.

In the following we will explore the full angular correlations of D-mesons defined by

$$\Delta\phi = \cos^{-1}(\vec{u} \cdot \vec{v}) / (|\vec{u}| \cdot |\vec{v}|). \quad (5)$$

Our results are shown in Fig. 3.

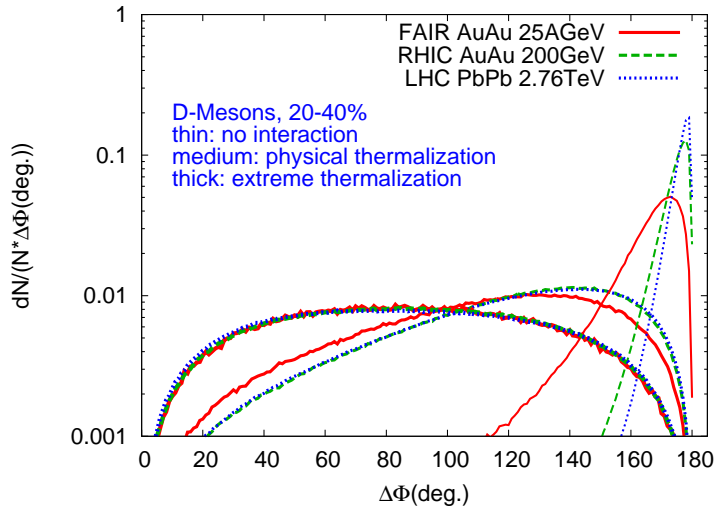


FIG. 3. (Color online) Angular correlations of D-mesons at FAIR, RHIC and LHC energies in the centrality range of 20-40%. Three different scenarios are shown: no interaction with the medium, physical drag and diffusion coefficients and extreme thermalization with 20-fold higher coefficients. The correlation gets flatter for lower collision energies and larger drag and diffusion coefficients. The angular modification for the case of no interaction is due to the coalescence mechanism. The yields are normalized to one.

Here, for random angular correlations the distribution corresponds to the geometrical $\sin \Delta\Phi$ dependence. As already seen in case of the azimuthal correlations, the correlations are moved to smaller angles for higher drag and diffusion coefficients. For the extreme thermalization scenario the D-mesons are preferably correlated with small angles due to the substantial radial and elliptic flow, as already seen in Fig. 2.

IV. THE INVARIANT MASS SPECTRA OF ELECTRONS FROM D-MESON DECAYS

As described in the introduction, electrons/positrons from $D\bar{D}$ -meson decays are the main background contribution for thermal QGP radiation in the invariant mass region of 1 to 3 GeV. Therefore, these invariant mass spectra will be explored for FAIR, RHIC and LHC energies in the following. Finally, the invariant mass spectrum at RHIC energy will be compared to available data.

To obtain these invariant mass spectra, we have described the decay of the (still correlated) D- and \bar{D} -mesons to e^+e^- pairs using PYTHIA. Our results are shown in Fig. 4.

Again the results for the three different energies assuming no thermalization, normal thermalization and extreme thermalization are shown. As expected the invariant mass spectra are softer for lower collision energies. At all energies the different thermalization scenarios lead to considerably different results. High thermalization leads to a strong suppression of high momentum particles, and the spectra become softer. In contrast to our calculations for the angular correlation

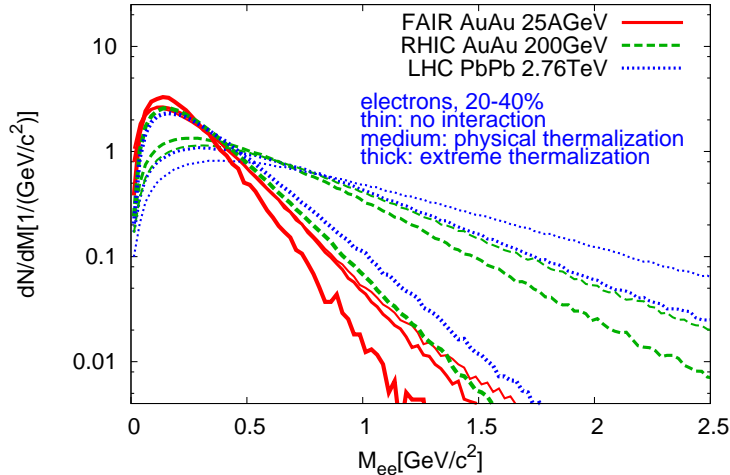


FIG. 4. (Color online) Invariant mass spectra of electrons from D-meson decays at FAIR, RHIC, and LHC energies in the of 20-40% centrality class. Three different scenarios are shown: no interaction with the medium, physical drag and diffusion coefficients and extreme thermalization with 20-fold higher coefficients. The spectra are harder for higher collision energies. Thermalization leads to considerably softer invariant mass spectra. The yields are normalized to one.

we see differing results for the different collision energies also when applying the full thermalization scenario. The reason are the higher momenta of the D-mesons at higher collision energies which translate to harder decay spectra.

Finally we compare our calculation to an experimentally measured invariant-mass spectrum from the PHENIX experiment at RHIC. Here we have performed a minimum bias calculation ($\sigma/\sigma_{\text{tot}} = 0\%-92\%$) and applied the appropriate experimental cuts. The result is shown in Fig. 5.

Here especially the $M_{\ell+\ell^-}$ range between the ϕ - and J/Ψ peak of ~ 1 to 3 GeV is of large interest because thermal dilepton radiation from the hot and dense matter is expected to dominate among all other thermal sources in this range. Our UrQMD calculation excluding interactions of the charm quarks with the medium approximately matches the measured dilepton radiation in the range of 1 to 3 GeV. If we include interactions of the charm quarks with the medium in the calculation (physical thermalization scenario) our result well underestimates the experimental data. This difference between the dilepton contribution of D-meson decays and the experimental dilepton measurements might originate from thermal radiation and might therefore be a QGP signal. It increases significantly in the dilepton mass range from 1 to 3 GeV. For completion we also included our calculation for extreme thermalization. Here high invariant masses are strongly suppressed and the difference between our calculation and the measured data is substantial in the invariant mass range of interest.

The difference of our calculation excluding interactions and the pp calculation in PYTHIA is, besides the hadronization mechanism, due to the different initial charm-quark distributions used. The random correlation that is used by the PHENIX collaboration assumes a flat angular correlation in contrast to the results of the calculation (cf. Fig. 3).

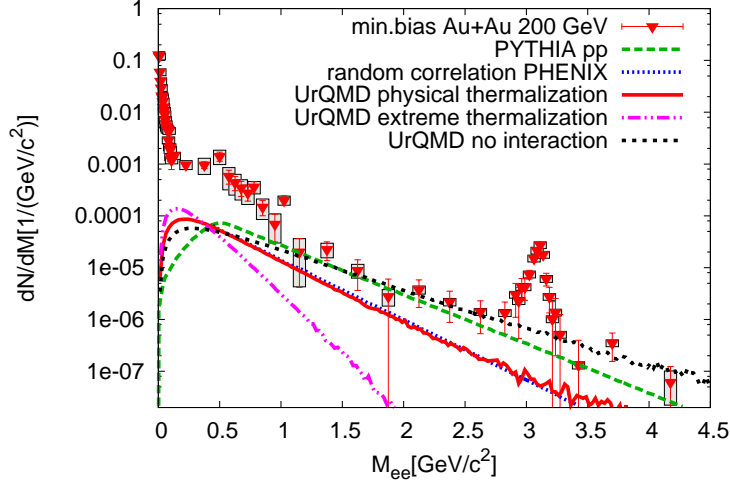


FIG. 5. (Color online) Invariant mass spectra of electrons in Au+Au collisions at $\sqrt{s_{NN}} = 200$ GeV in the centrality range of 0-92% (min. bias). A rapidity cut of $|y| < 0.35$ and a momentum cut of $p_T^e = 0.2$ GeV/c are applied. The dilepton data points are taken from a PHENIX measurement [56]. They are compared to calculations of electrons from D-meson decays. Also the pp calculation in PYTHIA and the random correlation calculation are taken from PHENIX [56]. The UrQMD calculations show three different scenarios: no interaction with the medium, physical drag and diffusion coefficients and extreme thermalization with 20 times higher coefficients. The difference between our physical scenario and the measured dilepton decays might be due to thermal radiation from the medium. The yields are normalized to the PYTHIA pp yield taken from [56].

V. SUMMARY

In this paper we have calculated the angular correlations of D-mesons and the invariant-mass spectra of e^+e^- pairs from correlated D- and \bar{D} -meson decays using a Langevin simulation within the UrQMD hybrid model for the bulk-medium evolution at FAIR, RHIC and LHC energies. For these calculations we have assumed a scenario without interactions of charm quarks with the medium, a physical scenario with realistic drag and diffusion coefficients (providing a satisfactory description of data on the R_{AA} and v_2 of non-photonic electrons at RHIC and D-mesons at LHC) and a scenario of extreme thermalization with strongly enhanced drag and diffusion coefficients.

The azimuthal correlation distributions show a flattening of the distribution function for higher drag and diffusion coefficients as predicted in an earlier calculation [4]. For an extreme thermalization, however, the correlation function tends to small angles due to the radial and elliptic flow developing in our hydrodynamic calculation. This effect can also be observed when exploring the full angular correlation distribution.

Subsequently, we have studied the invariant mass spectra of the electrons from D-meson decays and find softer spectra for low collision energies. Moreover the spectra show a considerably softer shape in case of stronger heavy-flavour-medium interactions.

Finally we have compared our calculations to experimental data from the PHENIX experiment. Here we find that our physical scenario cannot saturate the dilepton radiation in the dilepton invariant mass range between 1 and 3 GeV as a single source. We deduce that the difference between the experimental measurement and our calculation might be due to thermal radiation of the hot medium and might therefore originate from thermal QGP radiation.

We conclude, that a measurement of the angular correlation function would allow to check the validity of our model approach for D-meson correlations and therefore directly lead to a more

definite estimation of the QGP background radiation.

VI. ACKNOWLEDGMENTS

We are grateful to the Center for Scientific Computing (CSC) and the LOEWE-CSC at Frankfurt for providing computing resources. T. Lang gratefully acknowledges support from the Helmholtz Research School on Quark Matter Studies. This work is supported by the Hessian LOEWE initiative through the Helmholtz International Center for FAIR (HIC for FAIR). J. S. acknowledges a Feodor Lynen fellowship of the Alexander von Humboldt foundation. This work is supported by the Office of Nuclear Physics in the US Department of Energy's Office of Science under Contract No. DE-AC02-05CH11231, the GSI Helmholtzzentrum and the Bundesministerium für Bildung und Forschung (BMBF) grant No. 06FY7083.

-
- [1] J. Adams *et al.* (STAR Collaboration), Nucl. Phys. A **757**, 102 (2005), arXiv:nucl-ex/0501009 [nucl-ex].
 - [2] K. Adcox *et al.* (PHENIX Collaboration), Nucl. Phys. A **757**, 184 (2005), arXiv:nucl-ex/0410003 [nucl-ex].
 - [3] B. Muller, J. Schukraft, and B. Wyslouch, (2012), arXiv:1202.3233 [hep-ex].
 - [4] X. Zhu, M. Bleicher, S. Huang, K. Schweda, H. Stoecker, *et al.*, Phys. Lett. B **647**, 366 (2007), arXiv:hep-ph/0604178 [hep-ph].
 - [5] K. Schweda, X. Zhu, M. Bleicher, S. Huang, H. Stoecker, *et al.*, Braz.J.Phys. (2006), arXiv:nucl-ex/0610043 [nucl-ex].
 - [6] R. Rapp, Phys. Rev. C **63**, 054907 (2001), arXiv:hep-ph/0010101 [hep-ph].
 - [7] K. Gallmeister, B. Kampfer, and O. Pavlenko, Phys. Rev. C **57**, 3276 (1998), arXiv:hep-ph/9801435 [hep-ph].
 - [8] E. V. Shuryak, Phys. Rev. C **55**, 961 (1997), arXiv:nucl-th/9605011 [nucl-th].
 - [9] S. Bass, M. Belkacem, M. Bleicher, M. Brandstetter, L. Bravina, *et al.*, Prog. Part. Nucl. Phys. **41**, 255 (1998).
 - [10] M. Bleicher, E. Zabrodin, C. Spieles, S. Bass, C. Ernst, *et al.*, J. Phys. G **25**, 1859 (1999).
 - [11] D. H. Rischke, S. Bernard, and J. A. Maruhn, Nucl. Phys. A **595**, 346 (1995).
 - [12] D. H. Rischke, Y. Pursun, and J. A. Maruhn, Nucl. Phys. A **595**, 383 (1995).
 - [13] H. van Hees, M. Mannarelli, V. Greco, and R. Rapp, Phys. Rev. Lett. **100**, 192301 (2008).
 - [14] H. van Hees, V. Greco, and R. Rapp, (2007), arXiv:0706.4456 [hep-ph].
 - [15] V. Greco, H. van Hees, and R. Rapp, (2007), arXiv:0709.4452 [hep-ph].
 - [16] H. van Hees, M. Mannarelli, V. Greco, and R. Rapp, Eur. Phys. J. **61**, 799 (2009).
 - [17] R. Rapp, D. Cabrera, V. Greco, M. Mannarelli, and H. van Hees, (2008), arXiv:0806.3341 [hep-ph].
 - [18] R. Rapp and H. van Hees, (2008), published in The Physics of Quarks: New Research, Nova Publishers (Horizons in World Physics, Vol. 265) (2009), arXiv:0803.0901 [hep-ph].
 - [19] R. Rapp and H. van Hees, (2009), published in R. C. Hwa, X.-N. Wang (Ed.), Quark Gluon Plasma 4, World Scientific, p. 111, arXiv:0903.1096 [hep-ph].
 - [20] M. He, R. J. Fries, and R. Rapp, (2012), arXiv:1204.4442 [nucl-th].
 - [21] M. He, R. J. Fries, and R. Rapp, (2012), arXiv:1208.0256 [nucl-th].
 - [22] J. Aichelin, P. Gossiaux, and T. Gousset, (2012), arXiv:1201.4192 [nucl-th].
 - [23] J. Uphoff, O. Fochler, Z. Xu, and C. Greiner, Phys. Rev. C **84**, 024908 (2011).
 - [24] J. Uphoff, O. Fochler, Z. Xu, and C. Greiner, (2012), arXiv:1205.4945 [hep-ph].
 - [25] C. Young, B. Schenke, S. Jeon, and C. Gale, (2011), arXiv:1111.0647 [nucl-th].
 - [26] G. D. Moore and D. Teaney, Phys. Rev. C **71**, 064904 (2005).
 - [27] I. Vitev, A. Adil, and H. van Hees, J. Phys. G **34**, S769 (2007).
 - [28] P. Gossiaux, J. Aichelin, T. Gousset, and V. Guiho, J. Phys. G **37**, 094019 (2010).

- [29] P. B. Gossiaux, S. Vogel, H. van Hees, J. Aichelin, R. Rapp, M. He, and M. Bluhm, Phys. Rev. C (2011).
- [30] P. Gossiaux, J. Aichelin, and T. Gousset, Prog. Theor. Phys. Suppl. **193**, 110 (2012).
- [31] E. Bratkovskaya, O. Linnyk, V. Konchakovski, W. Cassing, V. Ozvenchuk, *et al.*, (2012), arXiv:1207.3198 [nucl-th].
- [32] O. Linnyk, W. Cassing, J. Manninen, E. Bratkovskaya, P. Gossiaux, *et al.*, (2012), arXiv:1208.1279 [nucl-th].
- [33] M. Nahrgang, J. Aichelin, P. B. Gossiaux, and K. Werner, (2013), arXiv:1305.3823 [hep-ph].
- [34] H. Petersen, J. Steinheimer, G. Burau, M. Bleicher, and H. Stöcker, Phys. Rev. C **78**, 044901 (2008).
- [35] S. Bass, A. Dumitru, M. Bleicher, L. Bravina, E. Zabrodin, *et al.*, Phys. Rev. C **60**, 021902 (1999).
- [36] A. Dumitru, S. Bass, M. Bleicher, H. Stoecker, and W. Greiner, Phys. Lett. B **460**, 411 (1999).
- [37] J. Steinheimer, M. Bleicher, H. Petersen, S. Schramm, H. Stöcker, *et al.*, Phys. Rev. C **77**, 034901 (2008).
- [38] J. Steinheimer, V. Dexheimer, H. Petersen, M. Bleicher, S. Schramm, *et al.*, Phys. Rev. C **81**, 044913 (2010).
- [39] H. Petersen, G.-Y. Qin, S. A. Bass, and B. Muller, Phys. Rev. C **82**, 041901 (2010).
- [40] H. Petersen, Phys. Rev. C **84**, 034912 (2011).
- [41] J. Steinheimer, S. Schramm, and H. Stöcker, Phys. Rev. C **84**, 045208 (2011).
- [42] B. Svetitsky, Phys. Rev. D **37**, 2484 (1988).
- [43] M. G. Mustafa, D. Pal, and D. Kumar, Srivastava, Phys. Rev. C **57**, 889 (1998).
- [44] H. van Hees, V. Greco, and R. Rapp, Phys. Rev. C **73**, 034913 (2006).
- [45] P. B. Gossiaux and J. Aichelin, Phys. Rev. C **78**, 014904 (2008).
- [46] M. He, R. J. Fries, and R. Rapp, Phys. Lett. B **701**, 445 (2011).
- [47] T. Lang, H. van Hees, J. Steinheimer, and M. Bleicher, (2012), arXiv:1211.6912 [hep-ph].
- [48] A. Bialas, M. Bleszynski, and W. Czyz, Nucl.Phys. **B111**, 461 (1976).
- [49] R. Glauber, (1987).
- [50] C. Spieles, R. Vogt, L. Gerland, S. Bass, M. Bleicher, *et al.*, Phys.Rev. **C60**, 054901 (1999), arXiv:hep-ph/9902337 [hep-ph].
- [51] M. L. Miller, K. Reygers, S. J. Sanders, and P. Steinberg, Ann.Rev.Nucl.Part.Sci. **57**, 205 (2007), arXiv:nucl-ex/0701025 [nucl-ex].
- [52] W. Cassing, E. Bratkovskaya, and A. Sibirtsev, Nucl. Phys. A **691**, 753 (2001), arXiv:nucl-th/0010071 [nucl-th].
- [53] T. Lang, H. van Hees, J. Steinheimer, and M. Bleicher, (2012), arXiv:1208.1643 [hep-ph].
- [54] T. Lang, H. van Hees, J. Steinheimer, Y.-P. Yan, and M. Bleicher, J.Phys.Conf.Ser. **426**, 012032 (2013), arXiv:1212.0696 [hep-ph].
- [55] T. Lang, H. van Hees, J. Steinheimer, and M. Bleicher, (2013), arXiv:1305.1797 [hep-ph].
- [56] A. Adare *et al.* (PHENIX Collaboration), Phys. Rev. C **81**, 034911 (2010), arXiv:0912.0244 [nucl-ex].